Geophysical Investigations of Rapid Tidewater Glacier Retreat

Shad O'Neel[1], Daniel E. McNamara[2] and W.Tad Pfeffer[1]
[1]*Institute of Arctic and Alpine Research, University of Colorado Boulder, Boulder CO 80309-0450, USA*
[2]*U.S.G.S. Golden, CO, 80401, USA*

IRIS Newsletter Article: DRAFT September 9, 2005

Glacier Climate Interaction

Although they comprise only 13% of the world's mountain glacier area (3% of total glacierized area of Earth), Alaskan and immediately adjacent Canadian glaciers supply one of the largest measured glaciological contributions to global sea level rise (~0.14 mm yr^{-1}, equivalent to new estimates from Greenland). Retreating tidewater glaciers dominate the Alaskan sea level contribution due to their ability to efficiently transfer mass via iceberg calving [*Arendt et al.*, 2002]. During retreat phase, a tidewater glacier may retreat on the order of 1-2 km yr^{-1} concurrent with dramatic increases in ice velocity. Catastrophic retreats of this style are thought to be irreversible [*Meier and Post*, 1987] until the terminus retreats to a position above local sea level. Comparatively, terrestrial glaciers, whose main mass loss mechanism is surface ablation, generally retreat on the order of 10 to several hundred m yr^{-1} and are reversible given adequate mass balance forcing.

Unlike their terrestrial counterparts, the relationship between climate and tidewater glaciers is complexly nonlinear; once initiated, tidewater glacier retreats proceed independently of the local climate. This is nicely illustrated by tidewater glaciers in south central and southeast Alaska, which all experience roughly the same climate. The tidewater glaciers of Glacier Bay initiated rapid retreat phases around the turn of the 20th century, while others, such as Columbia and LeConte Glaciers [*Krimmel*, 2001; *O'Neel et al.,* 2003], are currently undergoing rapid retreat. Contrarily, Taku and Hubbard Glaciers are slowly advancing [*Motyka et al.,* 2003].

[1]*Corresponding author address: Shad O'Neel; INSTAAR, University of Colorado, Boulder, 1560 30th St. Campus Box 450, Boulder CO, 80309, USA (303) 735-8167, email: shad@colorado.edu*

Rapidly Retreating Columbia Glacier

Columbia Glacier is located in south-central Alaska, approximately 30 km west of Valdez. The glacier flows 52 km from a maximum elevation of 3050 m down the flanks of the Chugach Mountains into Prince William Sound, where it terminates at a grounded ice cliff in deep water (Figure 1). The glacier attained a stable, shallow-water extended position (67 km long, 1100 km^2 surface area) at about 1100 A. D. and suffered only minor length and thickness changes until ca. 1980, after which time rapid retreat began [*Meier and Post,* 1987]. Since then, the terminus has retreated over 15 km concurrent with thinning exceeding 20 m a^{-1} at low elevations. The retreat is propagated by iceberg calving that exceeds incoming ice flux at an average rate of 0.74 km yr^{-1} [*O'Neel et al.*, 2005]. Although there has been a recent decline in retreat rate, which we attribute to a prominent constriction in the channel (Figure 1, near the 1999 terminus), discharge flux continues to greatly exceed the mass balance flux. Radio echo sounding measurements suggest that the glacier will retreat another ~15 km before the bed rises above sea level.

Columbia Glacier ranks among the world's fastest glaciers; surface speeds commonly exceed 25 m d^{-1}. Both observations of large amplitude, short period velocity variations (Figure 2) and calculations of internal deformation rates indicate that the flow is predominantly by basal sliding.

Field Studies

In order to study the role of calving in the dynamics of Columbia Glacier, we made measurements with a variety of geophysical instrumentation around the lower 20 km of the glacier channel. An array of ten high-frequency (1 Hz) Mark L22 seismometers and one broadband (0.33-30Hz) Guralp 40T seismometer were deployed on rock outcrops at the glacier margin during June 2004 for a period one-year (Figure 3). The array recorded over 100 Gbytes of continuous data at a rate of 100 $sampless^{-1}$ that included local and teleseismic earthquakes, small local seismic events generated by the glacier (icequakes), and four explosions detonated in boreholes on the glacier. Seismometers, power systems and recording equipment were obtained through the IRIS consortium's PASSCAL program.

The seismic experiment is one component of a larger integrated approach that addresses the problem of the role of calving in glacier dynamics. Additional field studies include:

- Measurements of ice motion using both high precision GPS (equipment supplied by UNAVCO) and optical surveying methods. Measurements of surface motion 7 km upstream from the terminus were made from June through Sept. 2004 (Figure 2) and motion near the terminus was measured for 25 days during June 2005. Additional GPS surveys measured short-term-average speeds at several locations and established a geodetic control network for photogrammetric analysis.
- Repeat aerial photography, extending from 1976 to the present used to determine glacier geometry and surface velocity fields.
- Terrestrial time-lapse photography (4 images d^{-1}) of the terminus (see http://tintin.colorado.edu/group/columbia/TLC.avi), which, using single camera photogrammetric techniques, provides a time series of volume change near the terminus.
- Bathymetry, water temperature and conductivity (salinity) measurements in newly exposed regions of the fjord to infer channel geometry and water discharge rates and patterns emanating from the sub-marine terminus.
- Detailed calving observations including timing, style, location, and subjective magnitude of thousands of calving events, used to ground truth the seismic records.
- Hourly surface air temperature and precipitation measurements, used to investigate forcing mechanisms for the time distribution of calving.

Integrated Data Analysis

Three primary goals of this experiment are documenting mechanical fracture processes involved in calving (including the location, rupture style, and seismic energy release), understanding the relationship between ice motion and calving and correlating ice motion and calving with possible forcing mechanisms. Previous studies have identified three characteristic seismic waveforms associated with three different icequake event types [e.g. *Qamar*, 1988; *Deichmann et al.,* 2000]. These include: 1. Calving events (low frequency, long duration, non-impulsive onsets, surface waves); 2. basal sliding (low frequency, short duration, no surface waves); and 3. surface crevassing (high frequency, short duration, impulsive onsets). *Qamar*'s (1988) work was performed at Columbia Glacier, when the glacier extended 10 km further down fjord, and provides a baseline for our work.

Calving events span a broad range of style and magnitude, ranging from small isolated pieces of ice dropping from the ice cliff to the water to large (1 km x 1 km) slabs rising up from great depths below the ocean surface (Figure 4a). *Qamar* (1988) showed that the duration of a seismic signal associated with calving correlates with ice volume however, amplitude does not. The position of their camp made differentiation of calving style and determination of ice volume challenging. Using our calving observations and seismic record from the broadband sensor located near the terminus, we intend to characterize the seismic waveforms (Figure 4b) associated with the primary calving styles and formulate an ice volume relationship using event amplitude, frequency content and duration.

Typically calving is thought of as a process occurring immediately at the terminus of a tidewater glacier. However, observations of along-flow strain rates indicate that failure processes may be operating significantly upstream of the terminus [*O'Neel et al.*, 2003]. Accurate calculations of icequake locations will allow us to investigate this idea. We detonated four explosions of varying magnitude at known locations on the glacier to determine seismic velocities in the local bedrock, which will allow us to more accurately determine icequake locations.

Rupture style will also be used to differentiate events generated by calving, crevassing or basal processes.

Our second primary goal is to investigate the relationship between the rate of calving and ice speed. Early predictions of the retreat grossly over-estimated retreat rates, primarily because researchers did not anticipate the large increase in surface speed as the terminus began to retreat. Classically, the calving rate U_c is a derived quantity, calculated as the difference between ice speed at the terminus U_i and change in glacier length dL/dt:

$$U_c = U_i - \frac{dL}{dt}$$

Ice speed and length change are typically measured photogrammetrically [e.g. *Krimmel*, 2001]. Our seismic data allow an independent determination of the calving rate (and potentially calving flux) that can be compared to photogrammatic measures of ice speed and length change.

For our final goal, we will identify statistical relationships between icequake occurrence (seismicity) and possible forcing mechanisms such as ice motion, tidal variations, temperature and precipitation.

Preliminary results suggest that calving events generate unique seismic records (Figure 4) that are distinguishable from earthquakes and other events generated by the glacier due to crevassing and basal sliding. The characteristic frequency of calving events is 1-3 Hz (Figure 4). Submarine calving events contain more low frequency energy than subaerial events . In addition to calving, two other event types were recorded; one has a characteristic frequency much lower than calving in the range of 0.05 – 0.1 Hz and may be related to basal sliding or sub-glacial hydraulics, while the second has a higher frequency content and shorter duration (< 1 sec) and is related to crevassing. Preliminary analysis of the GPS and seismic datasets indicates that overall icequake seismicity increases during speed-up events (Figure 2). Our ability to identify and separate icequake types by frequency content will enable us to investigate how calving and retreat are related to external driving processes.

Columbia Glacier demonstrates that ice loss from calving is a critical component in global sea level rise. Analogous, but larger and more rapid, retreat processes are presently underway at several major outlet glaciers of the Greenland Ice Sheet [*Joughin et al.,* 2004; *Krabill et al.,* 2004]. Rapid retreats result in a substantial new component to global sea level rise and provide strong motivation for a quantitative understanding of calving and rapid ice flow which control such catastrophic retreats. Our multidisciplinary investigations at Columbia glacier will provide a significant new contribution to our understanding of mechanical controls on marine terminating glacier instabilities including but not limited to climate triggering.

Acknowledgements

This work was supported by NSF OPP 0327345. We thank Tim Parker, Mary Templeton, Eliana Arias, and Bruce Beaudoin from PASSCAL for invaluable help in the field and with data formatting and timing corrections. Jake Walter, Ellie Boyce, H.P. Marshall and James McCreight provided essential volunteer field support. Martin Truffer provided active source timing and developed the single camera photogrammetry code. Thomas Hart was essential in the blasting efforts. None of the work would have been possible without the steady hands of Jim Harvey (Air Logistics) and Jan Gunderson (ERA helicopters). This work was supported by the National Science Foundation through grant # NSF-OPP-03.

References

Arendt. A. A., K.A. Echelmeyer, W.D. Harrison, C.S. Lingle, and V.B. Valentine (2002), Rapid wastage of Alaskan glaciers and their contribution to rising sea level, *Science*, 297(5580), 382-386.

Deichmann, N., Ansorge, J., Scherbaum, F., Aschwanden, A., Bernardi, F., and Gudmundsson, G., (2000), Evidence for deep icequakes in an alpine glacier. *Ann. Glaciol.* 31, 85-90.

Joughin I., W. Abdalati and M. Fahnestock. (2004), Large fluctuations in speed on Greenland's Jakobshavn Isbrae Glacier, *Nature*, 432,608-610.

Krabill, W. and 12 others. (2004), Greenland ice sheet: increased coastal thinning, *Geophys. Res. Lttrs,* 31(L24402).

Krimmel, R. (2001). Photogrammetric data set, 1957-2000, and bathymetric measurements for Columbia Glacier, Alaska. USGS Water-Resources Investigations Report 01-4089, 40 pp.

Meier, M F. and A. Post. (1987). Fast tidewater glaciers. *J. Geophys. Res.,* **92**(B9), 9051-9058.

Motyka, R.J. and Echelemeyer, K.E. (2003) Taku Glacier (Alaska, U.S.A.) on the move again: active deformation of proglacial sediments. *J. Glaciol.* **49**(164), p. 50-58.

O'Neel, S., K.A. Echelmeyer, and R.J. Motyka (2003), Short-term variations in calving of a tidewater glacier: LeConte Glacier, Alaska. *J. Glaciol.,* 49(167),587-598.

O'Neel, S., Pfeffer, W.T., Krimmel, R.M., and Meier, M.F. (2005), Evolving force balance at Columbia Glacier, Alaska, during its rapid retreat, *J. Geophys. Res.*

Qamar, A. (1988) Calving icebergs: a source of low-frequency seismic signals from Columbia Glacier, Alaska. *J. Geophys. Res.,*93(B6),6615-6623.

Figures

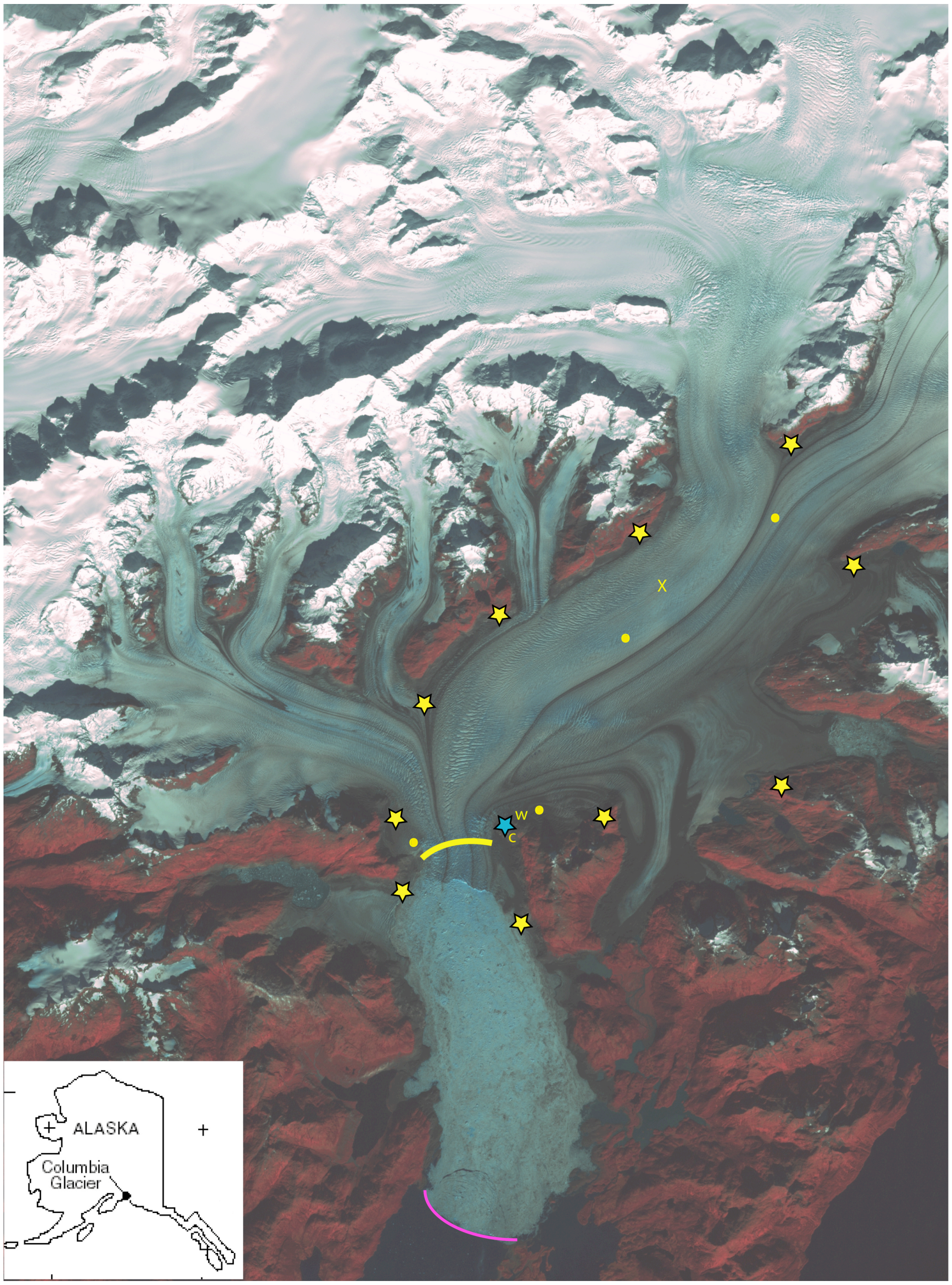

Figure 1. Lower Columbia Glacier as imaged by Landsat thematic Mapper on September 26, 1999. Stars mark the location of temporary seismic stations, yellow stars indicate Mark L-22 seismometers and the blue star shows the location of the Guralp 40-T broadband seismometer. The yellow w marks the location of weather observations, and the yellow c marks the time lapse camera. Explosion locations for the active source experiment are shown with yellow circles, and the location of the GPS receiver is marked with a yellow X. The 2004-2005 terminus position is roughly shown as a yellow line. The pre-retreat terminus position is shown in pink.

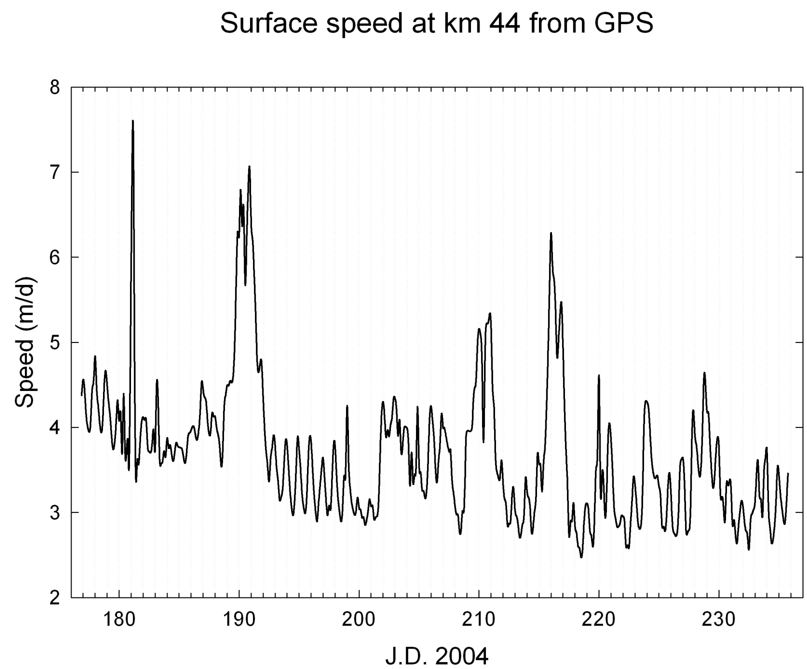

Figure 2. Horizontal velocity measured using high-precision GPS, approximately 7 km upstream of the 2004 terminus. (yellow X on figure 1).

Figure 3. Installing the broadband seismometer June 2004. Trimlines in the background show the pre-retreat ice thickness at this location. Photo by Tim Parker.

Figure 4. a) Seismogram of the calving event depicted in c. b) Spectragram for the hour during which the calving event took place. c) photographs of a large sub-marine calving event, with icebergs emerging from significant depth below sea level.